

## Entrainment of noise-induced and limit cycle oscillators under weak noise

Namiko Mitarai, Uri Alon, and Mogens H. Jensen

Citation: *Chaos* **23**, 023125 (2013); doi: 10.1063/1.4808253

View online: <http://dx.doi.org/10.1063/1.4808253>

View Table of Contents: <http://chaos.aip.org/resource/1/CHAOEH/v23/i2>

Published by the [American Institute of Physics](#).

---

### Additional information on Chaos

Journal Homepage: <http://chaos.aip.org/>

Journal Information: [http://chaos.aip.org/about/about\\_the\\_journal](http://chaos.aip.org/about/about_the_journal)

Top downloads: [http://chaos.aip.org/features/most\\_downloaded](http://chaos.aip.org/features/most_downloaded)

Information for Authors: <http://chaos.aip.org/authors>

### ADVERTISEMENT

AIP Advances

The logo for AIP Advances, featuring the text 'AIP Advances' in a blue and green font. Above the text is a decorative graphic of orange circles of varying sizes, some connected by a dotted line.

*Submit Now*

**Explore AIP's new  
open-access journal**

- **Article-level metrics  
now available**
- **Join the conversation!  
Rate & comment on articles**

# Entrainment of noise-induced and limit cycle oscillators under weak noise

Namiko Mitarai,<sup>1</sup> Uri Alon,<sup>2</sup> and Mogens H. Jensen<sup>1</sup>

<sup>1</sup>Niels Bohr Institute, University of Copenhagen, Blegdamsvej 17, Copenhagen 2100-DK, Denmark

<sup>2</sup>Weizmann Institute of Science, 234 Herzl St., Rehovot 76100, Israel

(Received 26 December 2012; accepted 16 May 2013; published online 7 June 2013)

Theoretical models that describe oscillations in biological systems are often either a *limit cycle oscillator*, where the deterministic nonlinear dynamics gives sustained periodic oscillations, or a *noise-induced oscillator*, where a fixed point is linearly stable with complex eigenvalues, and addition of noise gives oscillations around the fixed point with fluctuating amplitude. We investigate how each class of models behaves under the external periodic forcing, taking the well-studied van der Pol equation as an example. We find that when the forcing is additive, the noise-induced oscillator can show only one-to-one entrainment to the external frequency, in contrast to the limit cycle oscillator which is known to entrain to any ratio. When the external forcing is multiplicative, on the other hand, the noise-induced oscillator can show entrainment to a few ratios other than one-to-one, while the limit cycle oscillator shows entrainment to any ratio. The noise blurs the entrainment in general, but clear entrainment regions for limit cycles can be identified as long as the noise is not too strong. © 2013 AIP Publishing LLC. [<http://dx.doi.org/10.1063/1.4808253>]

**Biological systems present us with a wide range of oscillators, which include cell cycles, circadian rhythms, calcium oscillations, pace maker cells, and protein responses, but it is often a challenging task to identify the minimal models behind these oscillations. The proposed models are typically categorized into two classes: (i) *Limit cycle oscillator*, where fixed points are linearly unstable and the oscillations are described by stable limit cycles sustained by nonlinearities of the system which are deterministic. Noise can be added on the top of the deterministic oscillations. (ii) *Noise-induced oscillator*, where the fixed point is linearly stable for the system without noise and the system relaxes to the fixed point with damped oscillations when temporally perturbed. Addition of noise to this type of system is known to show sustained oscillations with fluctuating amplitudes. We propose a way to distinguish the two, by using the phenomenon of entrainment to a periodic perturbation. Taking the van der Pol equation with noise as an example, we show that entrainments to all the rational ratios are seen only in the limit cycle oscillator. In the case of the noise-induced oscillator with additive external forcing, the oscillator can entrain only at one-to-one ratio, meaning that the entrainment to other than the one-to-one ratio is the sign of the dominance of the limit cycle mechanism. When the external forcing is multiplicative, we find that the noise-induced oscillator with weak nonlinearity can show some entrainment ratios other than one-to-one, but not all the ratios.**

*oscillator*: The fixed point is linearly unstable, and the oscillations are described by stable limit cycles sustained by nonlinearity of the system in the deterministic case.<sup>11,12</sup> Noise (e.g., molecular noise due to limited number of copy numbers) can be added on the top of the deterministic oscillations. (ii) *Noise-induced oscillator*: The fixed point is linearly stable for the system without noise, and the system relaxes to the fixed point with damped oscillations when temporally perturbed. Addition of noise to such a system is known to show sustained oscillations with fluctuating amplitude.<sup>13,14</sup> For some systems, both limit cycle oscillators (i) and noise-induced oscillators (ii) are proposed as a mechanism for the oscillation.<sup>11–13</sup> Here, we propose a way to distinguish the two, by using the phenomenon of *entrainment* to a periodic perturbation.

It is well known that when an periodic perturbation is added to a deterministic limit cycle, the system's oscillation frequency  $\omega$  will be entrained to the external frequency  $\Omega$  with various rational numbers of frequencies  $\omega/\Omega = P/Q$  for all positive integers  $P$  and  $Q$  in a *finite window of the external frequency*  $\Omega$ , where the width of the window depends on the amplitude of the external forcing.<sup>15,16</sup> Entrainment, also called mode-locking, has been observed in variety of physical systems during the last decades, from onset of turbulence,<sup>17</sup> Josephson junctions,<sup>18,19</sup> one-dimensional conductors,<sup>20</sup> semiconductors,<sup>21,22</sup> and crystals.<sup>23</sup> It has been predicted and verified experimentally that the mode-locking structure possesses certain universal properties.<sup>15,16</sup> In biological systems, entrainment has been investigated theoretically for circadian rhythms<sup>4,5</sup> as well as in model systems for protein responses.<sup>25</sup> Experimental observation of entrainment in biological systems is often rather difficult due to noisy signals, but it has been observed for circadian rhythms<sup>2,3</sup> and synthetic genetic oscillators.<sup>24</sup>

In this paper, we study the difference in the entrainment behavior for the limit cycle oscillators and noise-induced oscillators. Our main question is the following: Can we

## I. INTRODUCTION

Biological systems present us with a bewildering fauna of oscillators: cell cycles,<sup>1</sup> circadian rhythms,<sup>2–5</sup> calcium oscillations,<sup>6</sup> pace maker cells,<sup>7</sup> protein responses,<sup>8–14</sup> and so on. Sometimes, however, it is hard to see what are the minimal models behind these oscillations. Typically, the models are categorized into two classes: (i) *Limit cycle*

distinguish the two cases by means of the entrainment behavior? We employ the famous van der Pol equation with noise as an example, because there we can easily study both cases by changing parameters. We show that entrainments to all the rational ratios are seen only in the limit cycle oscillator. In the case of the noise-induced oscillator with additive external forcing, the oscillator can entrain only at one-to-one ratio, meaning that the entrainment to other than the one-to-one ratio is the sign of the dominance of the limit cycle mechanism. When the external forcing is multiplicative, we find that the noise-induced oscillator with weak nonlinearity can show some entrainment ratios other than one-to-one, but not all the ratios. To confirm the generality of the entrainment behavior for the limit cycle system under weak noise, we also study a biological example, the tumor-necrosis factor (TNF)-driven oscillating nuclear factor- $\kappa$ B (NF- $\kappa$ B) system, and confirm that  $P/Q$  entrainments can be seen.

## II. MODEL

### A. van der Pol equation

Consider the following two-dimensional equation with noise

$$\dot{\mathbf{x}} = \mathbf{F}(\mathbf{x}) + \sigma \mathbf{\Gamma}, \tag{1}$$

with

$$\mathbf{x} = \begin{pmatrix} x_1(t) \\ x_2(t) \end{pmatrix}, \quad \mathbf{\Gamma} = \begin{pmatrix} \Gamma_1(t) \\ \Gamma_2(t) \end{pmatrix}, \tag{2}$$

$$\mathbf{F}(\mathbf{x}) = \begin{pmatrix} x_2(t) \\ -(Bx_1(t)^2 - d)x_2(t) - x_1(t) \end{pmatrix}. \tag{3}$$

Here  $d$ ,  $\sigma$ , and  $B$  are parameters, and  $\Gamma_i(t)$  are uncorrelated, statistically independent Gaussian white noise, satisfying

$$\langle \Gamma_j(t) \rangle = 0, \quad \langle \Gamma_j(t) \Gamma_k(t') \rangle = \delta_{j,k} \delta(t - t'). \tag{4}$$

First let us consider the deterministic case,  $\sigma = 0$ . The model has a fixed point at  $(x_1, x_2) = (0, 0)$ , and the eigenvalues around this fixed point are

$$\lambda_{\pm} = \frac{1}{2} (d \pm \sqrt{d^2 - 4}), \tag{5}$$

indicating that the system experiences a Hopf bifurcation at  $d=0$ . When  $d < 0$ , the fixed point relaxes to the fixed point with damped oscillation with the angular frequency  $\omega_{\ell}(d) = \sqrt{|d^2 - 4|}/2$ , while when  $d > 0$  and  $B > 0$  the model shows a stable limit cycle (van der Pol oscillator).

In the stochastic case with  $\sigma > 0$ , however, the system shows a sustained oscillation even in the linearly stable case,  $d < 0$ , because the noise keeps activating the oscillation with frequency  $\omega_{\ell}$ . This is the case of the linear p53 model introduced in Ref. 13. When  $d > 0$ ,  $\sigma > 0$  adds fluctuations on the top of the stable oscillation around the limit cycle.

### B. Setup

We investigate the entrainment behavior of the model, focusing on the following three classes of parameter sets.

1. The *limit cycle oscillator*, with  $d > 0$  and  $B > 0$ .
2. For the *noise-induced oscillator*, we consider the two subcategories.
  - (a) The *linear system with a stable fixed point*, with  $d < 0$  and  $B = 0$ , i.e., the equations are linear in  $\mathbf{x}$  and the fixed point is stable.
  - (b) The *nonlinear system with a stable fixed point*, with  $d < 0$  and  $B > 0$ , i.e., the fixed point is linearly stable but the equations possess a nonlinear term.

When noise-induced oscillators are studied, normally only linear terms are considered. However, in reality, there are often nonlinear terms, which can play a role when distance from the stable fixed point  $|\mathbf{x}|$  is sufficiently large. This is the reason why we consider both linear and nonlinear noise-induced oscillators.

When needed, numerical integration of stochastic differential equations are performed by using Euler method.

Figure 1 shows the typical behavior of the model in each categories. The parameters are chosen so that the period and amplitude are in similar range. Without noise, the limit cycle is the only case with stable oscillation (Fig. 1(a)), while linear and nonlinear systems with a stable fixed point exhibit damped oscillations relaxing to the fixed point (Figs. 1(b) and 1(c)). When noise is added, the oscillation is perturbed for limit cycle oscillator (Fig. 1(d)); here, the noise level is chosen so that the base oscillation is still recognizable. For linear and nonlinear noise-induced oscillators (Figs. 1(e) and 1(f)), we observe oscillations with the expected angular frequency ( $\omega_{\ell}(-0.1) \approx 1$ ). In order to demonstrate the difference between the two, we apply the exact same sequence of noises in both cases. We observe a bigger difference when linear noise-induced oscillator have large ( $|\mathbf{x}| \approx 1$ ) amplitude, because the nonlinear term becomes more important. Naturally this effect depends on the value of  $B$  (data not shown).

We study these oscillators under the following two kinds of external periodic perturbation.

#### 1. Additive forcing

The first case is an *additive* forcing, in the form of

$$\dot{\mathbf{x}} = \mathbf{F}(\mathbf{x}) + \sigma \mathbf{\Gamma} + \mathbf{A}(t), \tag{6}$$

with

$$\mathbf{A}(t) = \begin{pmatrix} 0 \\ A \end{pmatrix} \cos \Omega t. \tag{7}$$

#### 2. Multiplicative forcing

The second case is an *multiplicative* forcing (also called parametric forcing), in the form of

$$\dot{\mathbf{x}} = \mathbf{F}(\mathbf{x}) + \sigma \mathbf{\Gamma} + \mathbf{M}(t)\mathbf{x}, \tag{8}$$

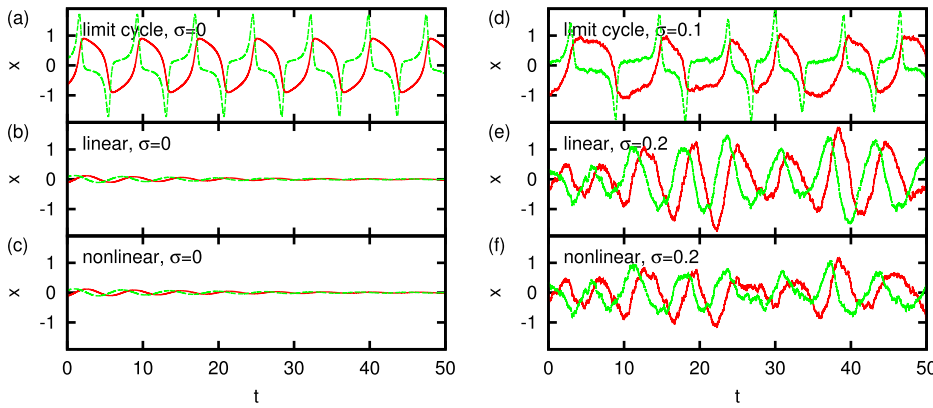


FIG. 1. The time evolution of  $x_1$  (solid line) and  $x_2$  (dashed line) when there is no external forcing. (a) Limit cycle oscillator with  $d=2$  and  $B=10$  without noise ( $\sigma=0$ ). (b) Linear system with  $d=-0.1$  and  $B=0$  without noise ( $\sigma=0$ ). (c) Nonlinear system with  $d=-0.1$  and  $B=1$  without noise ( $\sigma=0$ ). For (b) and (c), the initial condition is perturbed from the fixed point to demonstrate the damped oscillation. (d) Limit cycle oscillator with  $d=2$  and  $B=10$  with noise ( $\sigma=0.1$ ). (e) Linear system with  $d=-0.1$  and  $B=0$  with noise ( $\sigma=0.2$ ). (f) Nonlinear system with  $d=-0.1$  and  $B=1$  with noise ( $\sigma=0.2$ ).

where

$$\mathbf{M}(t) = \begin{pmatrix} 0 & 0 \\ M & 0 \end{pmatrix} \cos \Omega t. \tag{9}$$

In Sec. III, we first present the behavior of the model under the additive forcing and then show the parallel results for the multiplicative forcing.

### III. RESULTS

#### A. Additive forcing

##### 1. Linear case

In the case of the additive periodic forcing to a  $D$ -dimensional linear deterministic system, we have in general

$$\dot{\mathbf{x}}(t) = \mathbf{L}\mathbf{x}(t) + \mathbf{A}(t), \tag{10}$$

where  $\mathbf{L}$  is a coefficient matrix of the linearized equation and  $\mathbf{A}(t)$  is periodic function in time with a period  $T$ , satisfying  $\mathbf{A}(t+T) = \mathbf{A}(t)$ .

By expressing  $\mathbf{x}(t) = \sum_{j=1}^D C_j(t) \mathbf{u}_j$ , with using eigenvectors  $\mathbf{u}_j$  of the matrix  $L$  given by  $\mathbf{L}\mathbf{u}_j = \lambda_j \mathbf{u}_j$ , we can show that in the long-time limit we have

$$\lim_{t \rightarrow \infty} C_j(t) = \sum_{n=-\infty}^{\infty} \frac{F_n}{in \frac{2\pi}{T} - \lambda_j} e^{in \frac{2\pi}{T} t}. \tag{11}$$

Note that  $\Re(\lambda_j) < 0$  because the fixed point  $\mathbf{x} = 0$  is stable.  $F_n$  is defined by the Fourier expansion of  $\mathbf{A}(t)$  as

$$\mathbf{v}_j^t \cdot \mathbf{A}(t) = \sum_{n=-\infty}^{\infty} F_n e^{in \frac{2\pi}{T} t},$$

where  $\mathbf{v}_j^t$  is the left eigenvector. Therefore the solution will always be a periodic function of  $t$  with the period  $T$  in the long time limit and contains only the frequencies that the external forcing has. In other words, the system will be always in a 1/1 entrained state if the perturbation is pure sine or cosine wave.

When Gaussian white noise is added to Eq. (12), we have

$$\dot{\mathbf{x}}(t) = \mathbf{L}\mathbf{x}(t) + \mathbf{A}(t) + \sigma \Gamma(t). \tag{12}$$

In this case, we can evaluate the auto-correlation of  $C_j(t)$  for large enough  $t_0$  ( $t_0 \gg 1/|\Re \lambda_j|$ ) as

$$\begin{aligned} \langle C_j(t_0) C_j(t_0 + \tau) \rangle &\approx \sum_{n=-\infty}^{\infty} \sum_{n'=-\infty}^{\infty} \frac{F_n F_{n'}}{\left(in \frac{2\pi}{T} - \lambda_j\right) \left(in' \frac{2\pi}{T} - \lambda_j\right)} \\ &\times e^{i(n t_0 + n'(t_0 + \tau)) \frac{2\pi}{T}} - \frac{\sigma^2}{2\lambda_j} e^{-\lambda_j \tau}. \end{aligned} \tag{13}$$

Namely, the response contains oscillations with the frequencies from forcing  $2\pi/T$  and from the complex part of the eigenvalue  $\Im \lambda_j$ , and the amplitude of the latter is proportional to  $\sigma$ .

#### 2. Numerical results

We now investigate numerically the entrainment behaviors for all three categories. First we demonstrate the behavior without noise and then show how the noise modifies this behavior.

*a. Without noise.* Figure 2 illustrates typical entrainment behaviors for additive forcing when noise is absent. With a limit cycle oscillator (Figs. 2(a) and 2(d)), the system's angular frequency can entrain to the external angular  $\Omega$  with various ratios, while in the linear system, one-to-one entrainment occurs (Figs. 2(b) and 2(e)). The nonlinear system shows very similar behavior to the linear system, where we see only one-to-one entrainment (Figs. 2(c) and 2(f)).

In order to define the system's angular frequency in a simple way, we adopt the polar coordinate  $(r, \theta)$  using

$$x_1(t) = r(t) \cos \theta(t), \tag{14}$$

$$x_2(t) = r(t) \sin \theta(t), \tag{15}$$

as proposed in Ref. 26. We define  $\theta(t)$  so that  $(\theta(t) - \theta(0))/2\pi$  gives the winding number, i.e., how many times the orbit went around the fixed point by time  $t$ . The system's angular frequency is numerically calculated from

$$\omega = \frac{1}{T} [\theta(T) - \theta(0)] \tag{16}$$

for long enough  $T$  (typically 1000 times external forcing period). With this definition, Fig. 2(a) shows the entrainment of the ratio  $\omega/\Omega = 2/1$ , while Fig. 2(d) gives  $\omega/\Omega = 1/2$ .

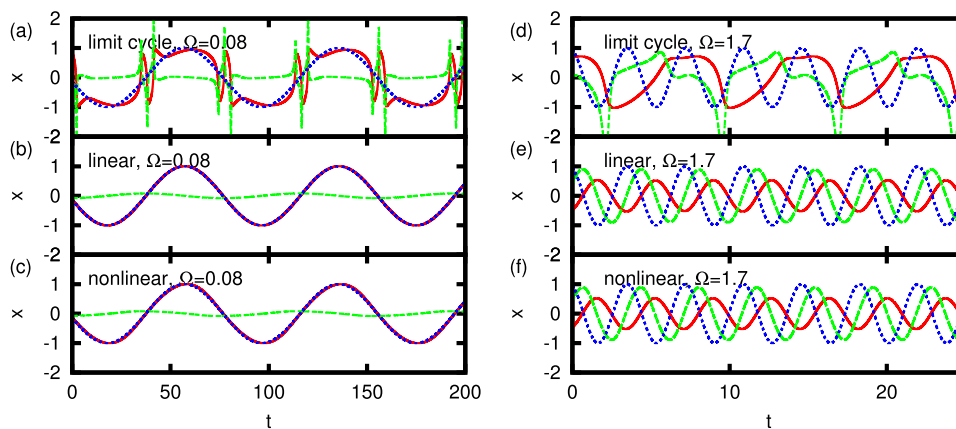


FIG. 2. The time evolution of  $x_1$  (solid line) and  $x_2$  (dashed line) when there is additive external forcing (dotted line,  $A = 1$ ). The external forcing has angular frequency  $\Omega = 0.08$  for (a)–(c), and  $\Omega = 1.7$  for (d)–(f). (a), (d) Limit cycle oscillator with  $d = 2$  and  $B = 10$  without noise ( $\sigma = 0$ ). (b), (e) Linear system with a stable fixed point with  $d = -0.1$  and  $B = 0$  without noise ( $\sigma = 0$ ). (c), (f) Nonlinear system with a stable fixed point with  $d = -0.1$  and  $B = 1$  without noise ( $\sigma = 0$ ). For the case with a limit cycle oscillator (a), (d), the system’s angular frequency can entrain to the external angular  $\Omega$  with various ratios, while in the linear and nonlinear systems with a stable fixed point case (b), (c), (e), (f) the system can only entrain to one to one ratio.

**b. With noise.** The addition of noise blurs the entrainment behavior, as depicted in Fig. 3. For the limit cycle oscillator (Figs. 3(a) and 3(d)), we can see that the noise makes the orbit irregular, which can make the phase to slip. In the linear noise-induced oscillator for small external angular frequency, we can clearly see that the noise induces the oscillation with angular frequency close to  $\omega_\ell$  on top of one-to-one entrainment behavior (Fig. 3(b)), as expected from the auto-correlation Eq. (13). When  $\Omega$  is larger than  $\omega_\ell$ , the external angular frequency is more visible, because the noise  $\sigma$  is small compared to the amplitude  $A$  for this case, although both frequencies should be present. The nonlinear noise-induced oscillator behaves again very similar to the linear case in entrainment behavior (Figs. 3(c) and 3(f)). The visible difference is a suppression of large amplitude by the nonlinear term.

**c. “Devil’s staircase” and “Arnold’s tongues.”** For deterministic limit cycles, the plot of  $\omega/\Omega$  vs  $\Omega$  for a fixed

amplitude of external forcing shows an infinitely complex structure with fractal nature, known as Devil’s staircase.<sup>15,16,26</sup> For the present system of limit cycle oscillator without noise, this is also observed as shown in Fig. 4(a) (solid line). As noise increases, the phase slips occasionally; therefore, narrow entrainment regions become harder to recognize (Fig. 4(a), dashed and dotted line). For the systems with a stable fixed point, there is only one-to-one entrainment for the no noise case (Fig. 4(b), solid line), while noise induced oscillation around the entrained solution will add some phase slips giving a change in the angular frequency when the entrainment is not so strong, resulting in an escape from the one-to-one ratio as shown in Fig. 4(b).

When entrainment regions for various values of  $\omega/\Omega$  are plotted in the  $A$ - $\Omega$  plain, it gives an “Arnold’s tongue” structure for the deterministic limit cycles: The entrainment regions widen as the external forcing amplitude  $A$  grows, resulting in tongue-like shapes of the entrainment region, when  $A$  is large enough the tongues start to overlap.<sup>15,16</sup> This

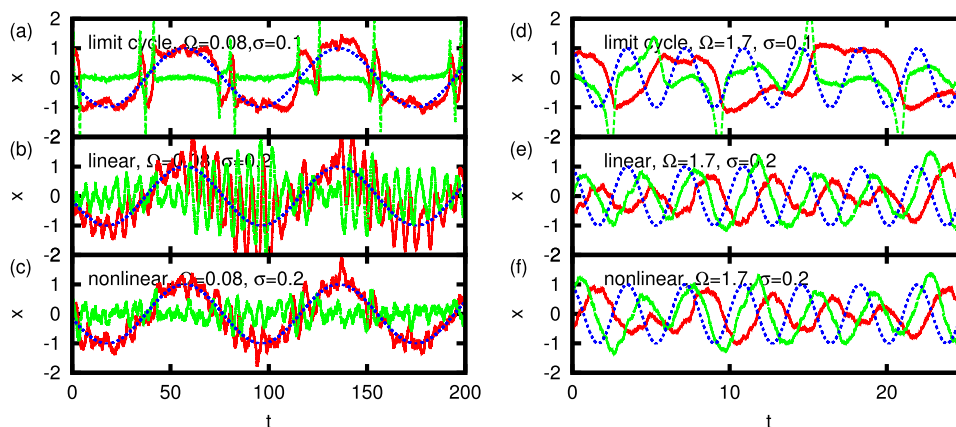


FIG. 3. The time evolution of  $x_1$  (solid line) and  $x_2$  (dashed line) when there is additive external forcing (dotted line,  $A = 1$ ). The external forcing has angular frequency  $\Omega = 0.08$  for (a)–(c), and  $\Omega = 1.7$  for (d)–(f). (a), (d) Limit cycle oscillator with  $d = 2$  and  $B = 10$  with noise ( $\sigma = 0.1$ ). (b), (e) Linear noise-induced oscillator with  $d = -0.1$  and  $B = 0$  with noise ( $\sigma = 0.2$ ). (c), (f) Nonlinear noise-induced oscillator with  $d = -0.1$  and  $B = 1$  with noise ( $\sigma = 0.2$ ). For the limit cycle oscillator (a), (d), the noise makes the orbit irregular, and the phase sometime slips. In the linear noise-induced oscillator for small external angular frequency, we can clearly see that the noise put the oscillation with angular frequency close to  $\omega_\ell$  on top of one-to-one entrainment behavior (b). When  $\Omega$  is larger than  $\omega_\ell$  (e), the external angular frequency is more visible, due to the smaller noise compared to the amplitude. The nonlinear noise-induced oscillator behaves again very similar to the linear case in entrainment behavior (c), (f), except for the suppression of large amplitude.

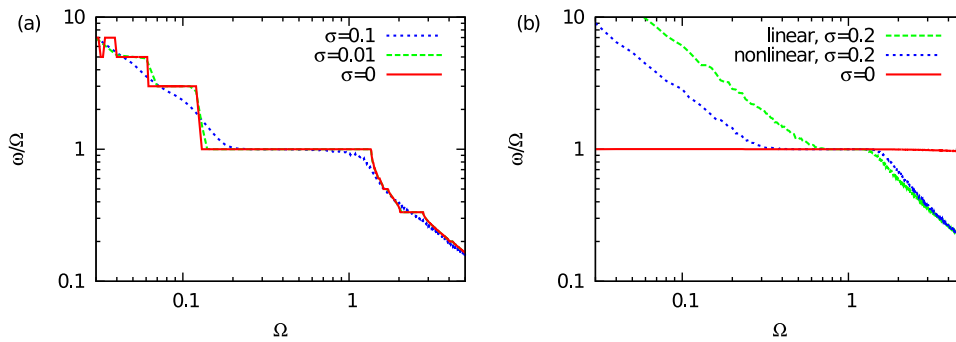


FIG. 4. “Devil’s staircase” for limit cycle oscillator (a) and linear and nonlinear systems with a stable fixed point (b) under additive forcing with  $A = 1$ . (a) The limit cycle oscillator with  $d = 2$  and  $B = 10$  with  $\sigma = 0.01$  (dotted line),  $\sigma = 0.1$  (dashed line), and  $\sigma = 0$  (solid line). (b) The systems with a stable fixed point ( $d = -0.1$ ). For the case without noise  $\sigma = 0$  (solid line), both linear ( $B = 0$ ) and nonlinear ( $B = 1$ ) systems show only one-to-one entrainment. With noise, the noisy oscillations around the one-to-one entrained orbit is induced, as shown with  $\sigma = 0.2$  (linear case with  $B = 0$  is shown by dashed line, and nonlinear case with  $B = 1$  is shown by dotted line).

can be seen in the limit cycle oscillator without noise in Fig. 5(a). When noise is added, the phase of the oscillator sometimes slips, resulting in narrower tongues (Fig. 5(b)). For the noise-induced oscillators (i.e., with a stable fixed point), there exists only 1/1 entrainment without noise, and with noise 1/1 entrainment is the only case that gives the tongue-like structure, both for the linear and nonlinear cases (Figs. 5(c) and 5(d)). We see other ratios of entrainment “regions” because for a given  $A$  with changing  $\Omega$ ,  $\omega/\Omega$  changes continuously outside of the entrainment region (e.g., Fig. 4(b)).

**B. Multiplicative forcing**

**1. Linear case without noise**

We next consider the multiplicative forcing

$$\dot{x}(t) = \mathbf{L}x(t) + \mathbf{M}(t)x(t), \tag{17}$$

where the matrix  $\mathbf{M}(t)$  satisfies

$$\mathbf{M}(t + T) = \mathbf{M}(t) \tag{18}$$

with  $T = 2\pi/\Omega$ . It is known from Floquet theory<sup>27</sup> that the solution matrix of this equation is expressed as

$$\mathbf{Q}(t) = e^{\mathbf{A}t}\mathbf{U}(t), \tag{19}$$

where

$$\mathbf{U}(t + T) = \mathbf{U}(t), \tag{20}$$

and a general solution is the linear combinations of column vectors consisting of  $\mathbf{Q}(t)$ . The eigenvalues of the matrix  $\mathbf{A}$ , called Floquet exponents, determine the stability of the solution: The solution will converge to the fixed point when the real parts of the Floquet exponents are all negative and diverges if some Floquet exponent have positive real parts. Therefore, no entrainment behavior will be observed for a linear noise-induced oscillator without noise under multiplicative forcing.

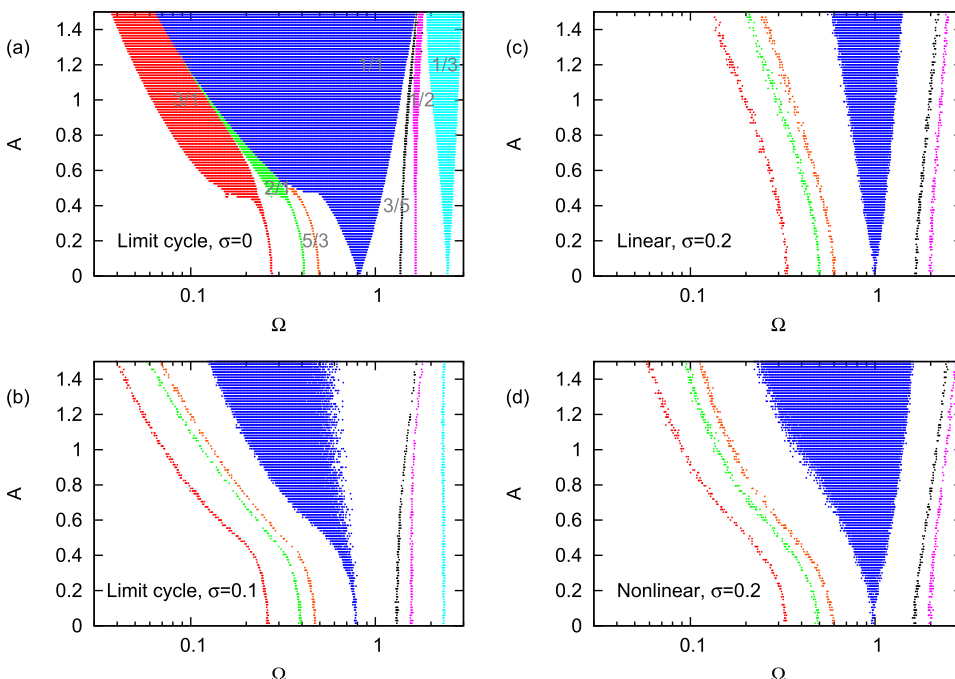


FIG. 5. “Arnold’s tongue” with additive forcing for limit cycle oscillator without (a) and with (b) noise and for noise-induced oscillator with noise for linear (c) and nonlinear (d) case. The horizontal axis is the external frequency  $\Omega$ , and the vertical axis is the forcing amplitude  $A$ . Entrainment is defined as  $\omega/\Omega$  is within 1% of the given value. (a) The limit cycle oscillator with  $d = 2$  and  $B = 10$  with  $\sigma = 0.0$ , which shows standard “Arnold’s tongue.” Noise ( $\sigma = 0.1$ ) make phases to slip, resulting in smaller region of entrainment (b). For noise induced oscillator with noise (c:  $d = -0.1, B = 0, \sigma = 0.2$ , d:  $d = -0.1, B = 1, \sigma = 0.2$ ), the tongue-like triangle structure is observed only for 1/1 entrainment.

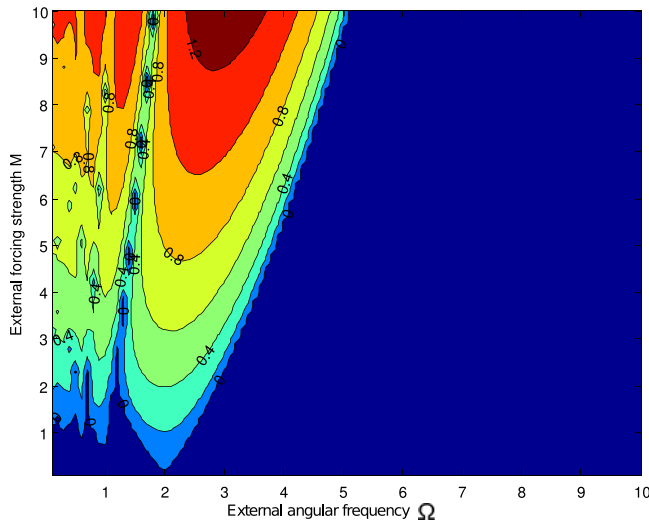


FIG. 6. Maximum real part of the Floquet exponent  $\lambda_R$  for various  $M$  and  $\Omega$ , for the linear system with stable fixed point ( $d = -0.1$  and  $B = 0$ ) without noise ( $\sigma = 0$ ).

In Fig. 6, we show numerically calculated the maximum real part of the Floquet exponents  $\lambda_R$  for Eq. (17) with Eq. (9) with  $d = -0.1$  and  $B = 0$ , as a function of amplitude of forcing  $M$  and external frequency  $\Omega$ . When  $\lambda_R < 0$  (dark blue region),  $|x|$  will exponentially decay to zero; otherwise,  $|x|$  will diverge except for the marginal case  $\lambda_R = 0$ .

## 2. Numerical results

*a. Without noise.* Figure 7 shows the entrainment behaviors for multiplicative forcing. For the limit cycle oscillator (Figs. 7(a) and 7(c)), there is no qualitative difference from the additive noise case, i.e., the system shows entrainment with various frequency ratio  $\omega/\Omega = P/Q$ . For the linear system with a stable fixed point without noise, on the other hand, the system can either decay to the fixed point (Fig. 7(b)) or diverge (Fig. 7(d)), which can be predicted from the Floquet exponents (Fig. 6). When nonlinear term is added, it does not prevent the decay (Fig. 7(c)), but the

divergent behavior is suppressed, and system shows the entrainment behavior (Fig. 7(f)). The frequency ratio  $\omega/\Omega$  is not necessarily 1/1; the example in Fig. 7(f) gives  $\omega/\Omega = 3/2$ .

*b. With noise.* When noise is added, the behavior changes drastically in the noise-induced oscillators, as shown in Fig. 8. The noise can induce the oscillation with the angular frequency close to  $\omega_\ell$  for the case where the no-noise system would decay to the fixed point (Figs. 8(b) and 8(c)). On the other hand, in the linear noise-induced oscillator, adding noise does not prevent divergence (Fig. 8(e)). For the parameters where no-noise system would entrain, the noise blurs the entrainment due to occasional phase slip for both limit cycle oscillator (Figs. 8(a) and 8(c)) and nonlinear noise-induced oscillator (Fig. 8(f)).

*c. “Devil’s staircase” and “Arnold’s tongue.”* We also study the “Devil’s staircase” for the multiplicative forcing. For the limit cycle oscillator without noise, we again see proper devil’s staircase, where noise will blur the entrainment behaviors (Fig. 9(a)). For the noise-induced oscillators, only the nonlinear case is studied because the linear case may diverge depending on the parameter values. Without noise, we see discrete finite regions of entrainment (Fig. 9(b) squares), while noise induces the oscillations in the decaying region resulting in a continuous line (Fig. 9(b) dashed line).

The Arnold’s tongue structure for the limit cycle is similar to those in the additive forcing case, as seen in Figs. 10(a) and 10(b). The Arnold’s tongues for all the entrainment ratios are observed without noise, and noise makes the regions smaller. For the nonlinear system with a stable fixed point without noise, there are entrainment regions for a few rational ratios, but the ones that appear are problem specific, for instance, in the present case, the  $\omega/\Omega = 1/3$  is not observed at all in Fig. 10(c). With noise (Fig. 10(d)), the entrainment regions shrinks, but at the same time the system can occasionally pass the given ratio of  $\omega/\Omega$ , resulting in narrow line of “fake” entrainment.

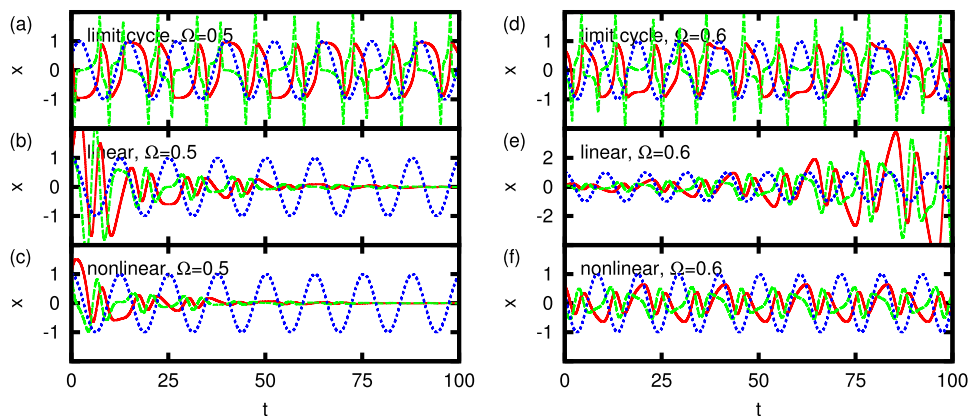


FIG. 7. Without noise: The time evolution of  $x_1$  (solid line) and  $x_2$  (dashed line) when there is multiplicative external forcing (dotted line,  $M = 1$ ). The external forcing has angular frequency  $\Omega = 0.5$  for (a)–(c), and  $\Omega = 0.6$  for (d)–(f). (a), (d) Limit cycle oscillator with  $d = 2$  and  $B = 10$  without noise ( $\sigma = 0$ ). (b), (e) Linear system with a stable fixed point with  $d = -0.1$  and  $B = 0$  without noise ( $\sigma = 0$ ). The transient behavior is shown. Note that the y-range in (e) is different from other plots. (c), (f) Nonlinear system with a stable fixed point with  $d = -0.1$  and  $B = 1$  without noise ( $\sigma = 0$ ). The limit cycle oscillator shows entrainments (a), (d), but the linear system either decays to zero (b) or diverges (e). The nonlinear system either decays (c) or entrains (f).

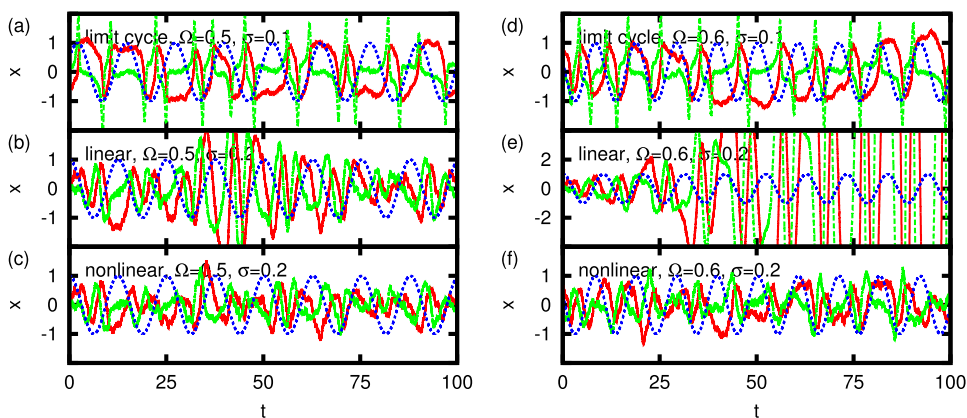


FIG. 8. With noise: The time evolution of  $x_1$  (solid line) and  $x_2$  (dashed line) when there is multiplicative external forcing (dotted line,  $M = 1$ ). The external forcing has angular frequency  $\Omega = 0.5$  for (a)–(c), and  $\Omega = 0.6$  for (d)–(f). (a), (d) Limit cycle oscillator with  $d = 2$  and  $B = 10$  with noise ( $\sigma = 0.1$ ). (b), (e) Linear noise-induced oscillator with  $d = -0.1$  and  $B = 0$  with noise ( $\sigma = 0.2$ ). Note that the y-range in (e) is different from other plots. (c), (f) Nonlinear noise-induced oscillator with  $d = -0.1$  and  $B = 1$  with noise ( $\sigma = 0.2$ ). The limit cycle oscillator shows entrainments with some phase slips (a), (d). For the linear and nonlinear system, the noise induces the oscillatory behavior, for the parameters where the system would decay without noise (b), (c).

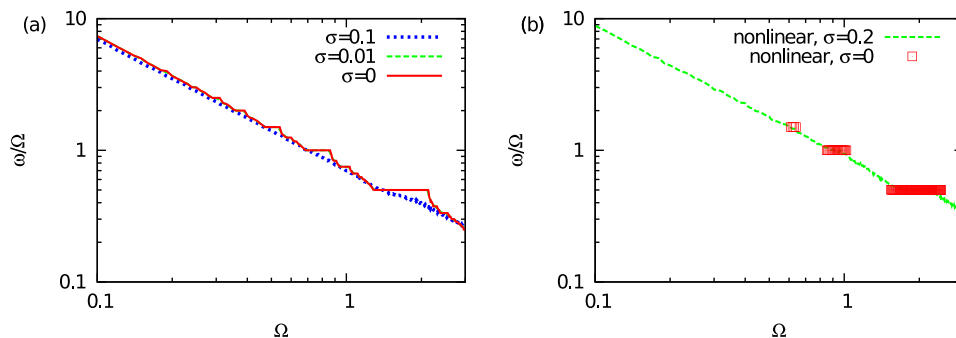


FIG. 9. “Devil’s staircase” for limit cycle oscillator (a) and nonlinear noise-induced oscillator (b) under multiplicative forcing with  $M = 1$ . (a) The limit cycle oscillator with  $d = 2$  and  $B = 10$  with  $\sigma = 0.01$  (dotted line),  $\sigma = 0, 1$  (dashed line), and  $\sigma = 0$  (solid line). (b) The nonlinear system with a stable fixed point with  $d = -0.1$  and  $B = 1$ . For the case without noise  $\sigma = 0$  (solid line), the decaying region where  $x$  goes to the fixed point is not shown, resulting in three discrete entrainment region. With noise, oscillation is induced in the decaying regime also, resulting in continuous line as shown for  $\sigma = 0.2$  (dashed line).

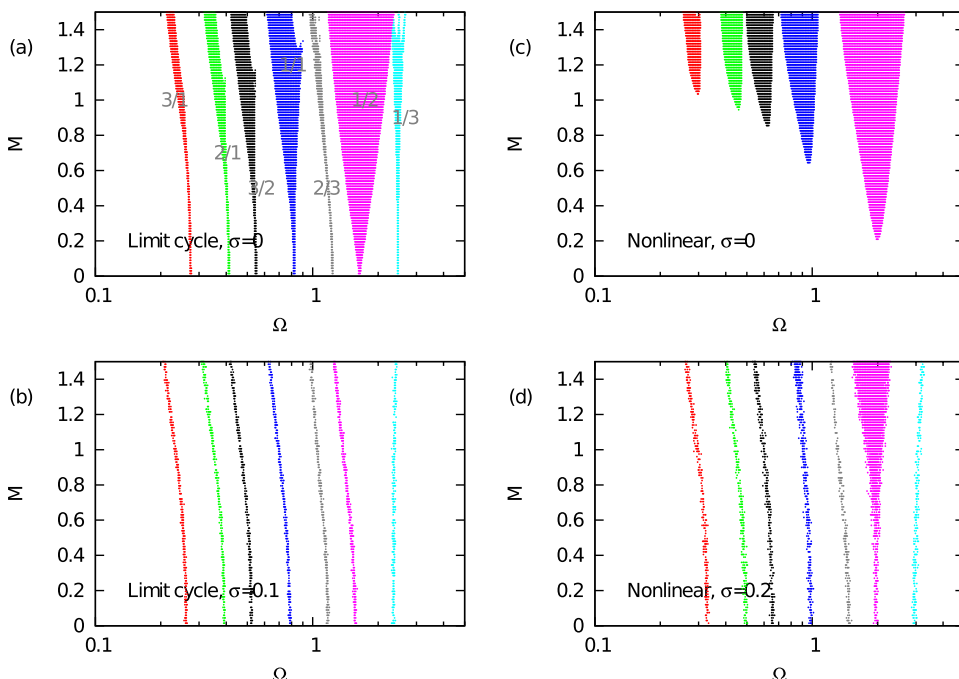


FIG. 10. “Arnold’s tongue” with multiplicative forcing for limit cycle oscillator without (a) and with (b) noise and for nonlinear system with a stable fixed point without (c) and with noise (d). The horizontal axis is the external frequency  $\Omega$ , and the vertical axis is the forcing amplitude  $M$ . Entrainment is defined as  $\omega/\Omega$  is within 1% of the given value. (a) The limit cycle oscillator with  $d = 2$  and  $B = 10$  with  $\sigma = 0$  shows standard “Arnold’s tongue,” while the noise ( $\sigma = 0.1$ ) makes the region of entrainment smaller (b). For nonlinear noise induced oscillator ( $d = -0.1, B = 1$ ) (c), there are a few entrainment regions for no noise case ( $\sigma = 0$ ), but not all the ratios are observed. For (c), the exponentially decaying case were excluded numerically by the following way: The equations are integrated with initial condition  $x(1) = 1$  and  $\dot{x}(2) = 0$ , and if the average amplitude for  $390\pi/\Omega < t < 400\pi/\Omega$  is less than 90% of the average amplitude for  $200\pi/\Omega < t < 210\pi/\Omega$ , then the solution is excluded.

**IV. BIOLOGICAL EXAMPLE: ENTRAINMENT OF TNF-DRIVEN NF-κB SYSTEM**

In this section, we study a biological example, TNF-driven NF-κB system, to confirm the generality of the entrainment behavior for the limit cycle system under weak noise.

The system has been studied for the deterministic case in Ref. 25. NF-κB is a transcription factor, and it has been verified experimentally that NF-κB level in the nucleus shows sharp oscillations after treatment with TNF.<sup>8,9</sup> The interaction network involves a negative feedback loop between the NF-κB and an inhibitor, IκBα, which is the main mechanism for the oscillations. TNF modulates the state of the IκBα and hence affects the oscillation. TNF can be added externally to the cell; therefore, it can serve as a possible probe to study the entrainment, i.e., we can use TNF level as the external forcing term. In Ref. 25, the system was modeled by 5 dimensional coupled nonlinear ordinary differential equations (ODEs)

$$\frac{dx}{dt} = F(x, [TNF]),$$

where

$$F_1 = k_{Nin}(N_{tot} - x_1) \frac{K_I}{K_I + x_3} - k_{lin}x_3 \frac{x_1}{K_N + x_1}, \tag{21}$$

$$F_2 = k_t x_1^2 - \gamma_m x_2, \tag{22}$$

$$F_3 = k_{it}x_2 - \alpha x_4(N_{tot} - x_1) \frac{x_3}{K_I + x_3}, \tag{23}$$

$$F_4 = k_a[TNF](I_{tot} - x_4 - x_5) - k_i x_4, \tag{24}$$

$$F_5 = k_i x_4 - k_p x_5 \frac{k_{A20}}{k_{A20} + A_{20}[TNF]}. \tag{25}$$

The variable  $x_1$  denotes the nuclear NF-κB level, and  $[TNF]$  denotes the TNF level, which we shall change to a periodically external forcing onto the system. The biological meaning of the variables and parameter values are summarized in Table I. Note that  $[TNF]$  appears twice in Eq. (25) in the terms multiplied with  $x$ ; therefore, this is an example of multiplicative forcing. We study this system with adding a Gaussian white noise in each term, i.e.,

$$\frac{dx}{dt} = F(x, [TNF]) + \sigma \Gamma.$$

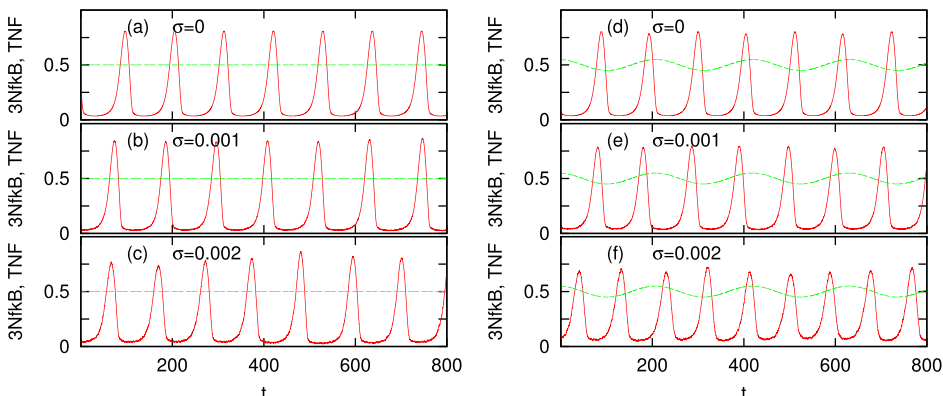


FIG. 11. The oscillations and entrainment for TNF-driven NF-κB system. The left panel shows spontaneous oscillations with  $[TNF] = 0.5$  for (a) no noise ( $\sigma = 0$ ) case and (b)  $\sigma = 0.001$ , (c)  $\sigma = 0.002$ . The right panel shows entrainments with  $M_{TNF} = 0.05$  and  $\Omega = 0.0297$  with (d) no noise ( $\sigma = 0$ ) case and (e)  $\sigma = 0.001$ , (f)  $\sigma = 0.002$ . Solid lines show  $3x_1$ , and dashed lines shows  $[TNF]$ .

TABLE I. Variables and the parameters in the TNF-driven NF-κB oscillation, from Ref. 25.

$x_1$	Nuclear NF-κB level
$x_2$	IκB mRNA level
$x_3$	Cytoplasmic IκB protein level
$x_4$	Active IKK level
$x_5$	Inactive IKK level
$N_{tot}$	Total NfκB level, 1 μM
$I_{tot}$	Total IKK level, 2.0 μM
$k_{Nin}$	5.4 min <sup>-1</sup>
$K_I$	0.035 μM
$k_{lin}$	0.018 min <sup>-1</sup>
$K_N$	0.029 μM
$k_t$	1.03 μM <sup>-1</sup> min <sup>-1</sup>
$\gamma_m$	0.017 min <sup>-1</sup>
$k_{it}$	0.24 min <sup>-1</sup>
$\alpha$	1.05 μM <sup>-1</sup>
$k_a$	0.24 min <sup>-1</sup>
$k_i$	0.18 min <sup>-1</sup>
$k_p$	0.036 min <sup>-1</sup>
$k_{A20}$	0.0018 μM
$A_{20}$	0.0028 μM

Figures 11(a)–11(c) show the spontaneous oscillation of nuclear NF-κB, when  $[TNF]$  is kept constant at  $[TNF] = 0.5$ , without (a) and with noise (b)–(c). We see clear periodic oscillation with the period around 110 (minutes). We then modulate the  $[TNF]$  level around this basal level<sup>25</sup> as

$$[TNF] = 0.5 + M_{TNF} \sin(\Omega t). \tag{26}$$

This has been studied in the no-noise case by Jensen and Krishna,<sup>25</sup> and it was found that the entrainments of various ratios can occur, when the frequency of the NF-κB level is determined based on the frequency of the peaks. Figure 11(d) shows an example of 1/2 entrainment, for  $M_{TNF} = 0.05$  and  $\Omega = 0.0297$ , in the deterministic case. With weak enough noise, the entrainment is maintained (Fig. 11(e)), but larger noise induces phase slips (Fig. 11(f)), as has been seen in the Van der Pol system.

In Fig. 12, several Devil’s staircases are shown with and without noise. In Ref. 25 the Arnold tongues have been calculated, and it has been demonstrated that general P/Q entrainments occur. A characteristic observation to this system is that the tongues overlap easier for larger external

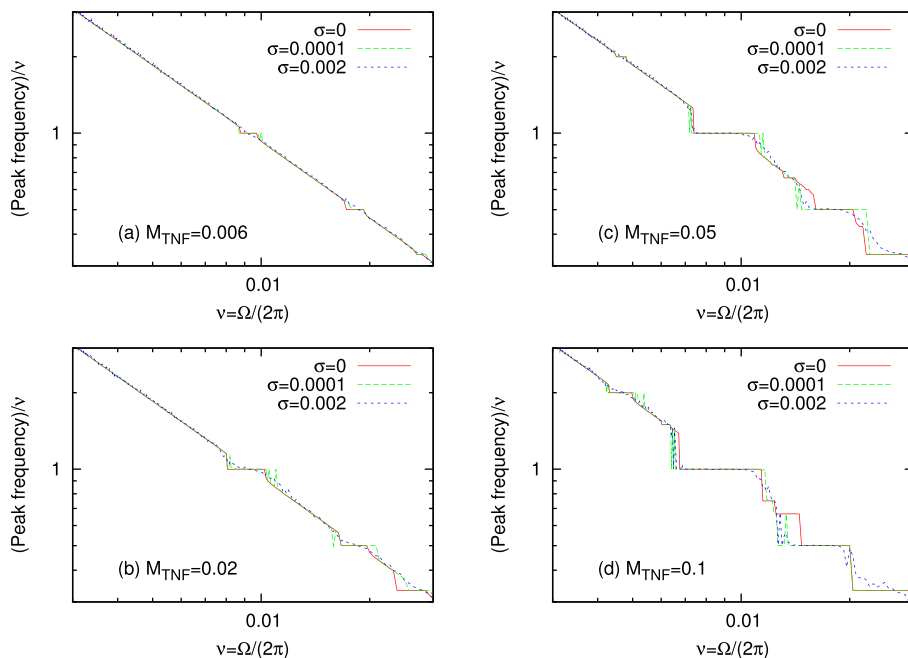


FIG. 12. “Devil’s staircase” for TNF-driven NF-κB system without and with noise, with (a)  $M_{TNF} = 0.006$ , (b)  $M_{TNF} = 0.02$ , (c)  $M_{TNF} = 0.05$ , and (d)  $M_{TNF} = 0.1$ . The entrainment regions are calculated from the frequency of the peaks in the deterministic case. In the finite noise case, we define the nuclear NF-κB peak as follows: We first determined the maximum value  $N_{max}$  and the minimum value  $N_{min}$  of  $x_1$  of the steady state in the deterministic simulation for the given parameters. We then calculate two thresholds,  $N_H = (N_{max} + N_{min})/2$  and  $N_L = (N_{max} + 3N_{min})/4$ . Next we perform the corresponding simulation with finite  $\sigma$ . We define a switching event from the “low” state to “high” state when  $x_1$  exceeds  $N_H$ , while the reverse switching happens when  $x_1$  becomes smaller than  $N_L$ . The number of peaks are calculated from how often the “high” states are reached. This way we can filter out the wiggly motion due to the noise and thus define the overall peak.

frequency; e.g.,  $M_{TNF} \approx 0.04$  for 1/3 and 1/2 tongues to overlap, while the 2/1 and 5/2 tongues do not overlap even at  $M_{TNF} = 0.1$ . When the Devil’s staircase are calculated for overlapping region, non-smooth or irregular jumps between the steps can be seen and is thus dependent on initial conditions in general. This is visible in our data in Fig. 12, for large  $M_{TNF}$  and larger  $\Omega$ . When weak noise is added, it enables the system to jump to other overlapping tongues, which results in irregular behavior around the entrainment regions. As the noise becomes larger, the entrainment is again smoothed away by phase slips.

**V. SUMMARY AND DISCUSSION**

Our motivation behind this work was to ask: Can one by applying an external periodic forcing and studying entrainment determine whether an oscillating system is driven by a linear mechanism (noise induced oscillator) or a non-linear mechanism (limit cycle oscillator)? Our answer to this question is generally yes. Our obtained results on entrainment behavior of oscillators are summarized in Table II.

When the forcing is additive, there is clear difference between the limit cycle oscillators and the noise-induced

oscillators. The former can entrain to any frequency ratio, while the latter shows only one-to-one entrainment. Therefore, if one see entrainment to  $P/Q \neq 1$  ratio, under additive forcing, it is a sign of limit cycle oscillator.

When the forcing is multiplicative, the non-linear noise-induced oscillators can also show  $P/Q \neq 1$  ratio entrainment, but not necessarily all of the rational ratios. If the system is noise-induced oscillator and the non-linear term is small, one might be able to capture the diverging tendency of the amplitude, because saturation happens when the amplitude is large enough to make the non-linear term relevant. In such a case, one might see big difference in amplitude for a fixed  $M$  with varying  $\Omega$ .

We thus urge experiment to be performed on oscillating biological systems. It is well known that some proteins (p53, NF-κB, Wnt) can oscillate in cells under stress responses. In the case of p53, both non-linear<sup>11,12</sup> and linear models have been proposed.<sup>13</sup> By applying an external time dependant signal such as DNA damaging radiation or drugs which specifically perturb the p53 circuit, it might be possible to entrain the internal oscillation and draw conclusions on the basis of our results summarized in Table II. In the case of

TABLE II. Summary of entrainment behavior of oscillators under additive and multiplicative forcing. A and M in the “force” column represent additive and multiplicative forcing, respectively.

Oscillator	No noise	With noise	Force
Limit cycle	Entrainment to any $P/Q$ Entrainment to any $P/Q$	Entrainment to any $P/Q$ with phase slips	A
		Entrainment to any $P/Q$ with phase slips	M
Linear	One-to-one entrainment <sup>a</sup>	One-to-one entrainment <sup>a</sup> with phase slips	A
Noise-induced	Decay or diverge	Noise-induced oscillation with $\sim \omega_\ell$ or diverge	M
Nonlinear	One-to-one entrainment <sup>a</sup>	One-to-one entrainment <sup>a</sup> with phase slips	A
Noise-induced	Small decay or Some $P/Q$ entrainment	Noise-induced oscillation with $\sim \omega_\ell$ or Some $P/Q$ entrainment with phase slips	M

<sup>a</sup>All the frequencies contained in the forcing can be observed.

NF- $\kappa$ B oscillations, one might be able to entrain the internal oscillation by an externally varying cytokine (like TNF) signal.<sup>25</sup> Potentially, it could lead to a way of controlling the DNA-repair pathway.

The present research also opens for further theoretical investigations. The  $P/Q \neq 1$  entrainment of the winding number for a nonlinear noise-induced oscillator with multiplicative forcing is a purely numerical observation, and further research is needed to refine the condition when this can occur. We did not study the strong noise case either, and it would be interesting to investigate in more details the active role of noise in the entrainments of limit cycles. In many biological examples, where dynamics are molecular reaction based, additive Gaussian white noise is not appropriate for large noise because it does not reflect the noise amplitude dependence on the molecule number: instead either a concentration dependent noise amplitude or a stochastic treatment of molecule numbers should be performed.

Finally, we would like to briefly comment on “noise-induced” oscillations by mechanisms other than the linear model studied here. It has been long known that when noise is added to excitable system with a stable fixed point, regular oscillatory behaviour can be observed at a certain level of noise (coherence resonance).<sup>28,29</sup> Since the nonlinearity plays an important role in an oscillation, such a system shows mode-locking behaviour similar to the deterministic nonlinear oscillators.<sup>30</sup> More recently, in gene network models with negative feedback, it has been shown that the noise due to finiteness of the number of molecules can modify the condition for oscillatory behaviour<sup>31</sup> or enhance the oscillation.<sup>32</sup> It would also be interesting to see the entrainment behaviour in such systems.

## ACKNOWLEDGMENTS

This study was supported by the Danish National Research Foundation through the Center for Models of Life.

<sup>1</sup>T. Y. Tsai, Y. S. Choi, W. Ma, J. R. Pomeroy, C. Tang, and J. E. Ferrell, Jr., *Science* **321**, 126–129 (2008).

<sup>2</sup>Q. Thommen, B. Pfeuty, P. E. Morant, F. Corellou, F. Y. Bouget, and M. Lefranc, *PLOS Comput. Biol.* **6**, e1000990 (2010).

<sup>3</sup>G. Asher, H. Reinke, M. Altmeyer, M. Gutierrez-Arcelus, M. O. Hottiger, and U. Schibler, *Cell* **142**, 943–953 (2010).

<sup>4</sup>B. Pfeuty, Q. Thommen, and M. Lefranc, *Biophys. J.* **100**, 2557–2565 (2011).

<sup>5</sup>C. Gérard and A. Goldbeter, *PLOS Comput. Biol.* **8**, e1002516 (2012).

<sup>6</sup>A. Goldbeter, *Nature (London)* **420**, 238–245 (2002).

<sup>7</sup>B. O'Rourke, B. M. Ramza, and E. Marban, *Science* **265**, 962–966 (1994).

<sup>8</sup>A. Hoffmann, A. Levchenko, M. L. Scott, and D. Baltimore, *Science* **298**, 1241–1245 (2002).

<sup>9</sup>D. E. Nelson, A. E. Ihekweaba, M. Elliott, J. R. Johnson, C. A. Gibney, B. E. Foreman, G. Nelson, V. See, C. A. Horton, D. G. Spiller, S. W. Edwards, H. P. McDowell, J. F. Unitt, E. Sullivan, R. Grimley, N. Benson, D. Broomhead, D. B. Kell, and M. R. White, *Science* **306**, 704–708 (2004).

<sup>10</sup>S. Krishna, M. H. Jensen, and K. Sneppen, *Proc. Nat. Acad. Sci. U.S.A.* **103**, 10840–10845 (2006).

<sup>11</sup>G. Tian, K. Sneppen, and M. H. Jensen, *Eur. Phys. J. B* **29**, 135–140 (2002).

<sup>12</sup>N. Geva-Zatorsky, N. Rosenfeld, S. Itzkovitz, R. Milo, A. Sigal, E. Dekel, T. Yarnitzky, Y. Liron, P. Polak, G. Lahav, and U. Alon, *Mol. Syst. Biol.* **2**, 2006.0033 (2006).

<sup>13</sup>N. Geva-Zatorsky, E. Dekel, E. Batchelor, G. Lahav, and U. Alon, “Fourier analysis and systems identification of the p53 feedback loop,” *Proc. Natl. Acad. Sci. U.S.A.* **107**, 13550 (2010).

<sup>14</sup>M. Lang, S. Waldherr, and F. Allgower, “Amplitude distribution of stochastic oscillations in biochemical networks due to intrinsic noise,” *PMC Biophys.* **2**, 10 (2009).

<sup>15</sup>M. Jensen, P. Bak, and T. Bohr, *Phys. Rev. Lett.* **50**, 1637–1639 (1983).

<sup>16</sup>M. Jensen, P. Bak, and T. Bohr, *Phys. Rev. A* **30**, 1960–1969 (1984).

<sup>17</sup>J. Stavans, F. Heslot, and A. Libchaber, *Phys. Rev. Lett.* **55**, 596–599 (1985).

<sup>18</sup>W. J. Yeh, D. R. He, and Y. H. Kao, *Phys. Rev. Lett.* **52**, 480 (1984).

<sup>19</sup>D. R. He, W. J. Yeh, and Y. H. Kao, *Phys. Rev. B* **31**, 1359–1373 (1985).

<sup>20</sup>S. E. Brown, G. Mozurkewich, and G. Gruner, *Phys. Rev. Lett.* **52**, 2277–2280 (1984).

<sup>21</sup>E. G. Gwinn and R. M. Westervelt, *Phys. Rev. Lett.* **57**, 1060–1063 (1986).

<sup>22</sup>A. Cumming and P. S. Linsay, *Phys. Rev. Lett.* **59**, 1633–1636 (1987).

<sup>23</sup>S. Martin and W. Martienssen, *Phys. Rev. Lett.* **56**, 1522–1525 (1986).

<sup>24</sup>O. Mondragon-Palomino, T. Danino, J. Selimkhanov, L. Tsimring, and J. Hasty, *Science* **333**, 1315–1319 (2011).

<sup>25</sup>M. H. Jensen and S. Krishna, *FEBS Lett.* **586**, 1664–1668 (2012).

<sup>26</sup>U. Parlitz and W. Lauterborn, *Phys. Rev. A* **36**, 1428–1434 (1987).

<sup>27</sup>H. Haken, *Advanced Synergetics: Instability Hierarchies of Self-Organizing Systems and Devices* (Springer-Verlag, Berlin, 1983), Chap. 2.

<sup>28</sup>H. Gang, T. Ditziinger, C. Z. Ning, and H. Haken, *Phys. Rev. Lett.* **71**, 807–810 (1993).

<sup>29</sup>A. S. Pikovsky and J. Kurths, *Phys. Rev. Lett.* **78**, 775–778 (1997).

<sup>30</sup>C. Zhou, J. Kurths, and B. Hu, *Phys. Rev. E* **67**, 030101(R) (2003).

<sup>31</sup>A. Loinger and O. Biham, *Phys. Rev. E* **76**, 051917 (2007).

<sup>32</sup>P. E. Morant, Q. Thommen, F. Lemaire, C. Vandermoëre, B. Parent, and M. Lefranc, *Phys. Rev. Lett.* **102**, 068104 (2009).